Eur. Phys. J. C (2011) 71:1640
DOI 10.1140/epjc/s10052-011-1640-3

THE EUROPEAN PHYSICAL JOURNAL C

Special Article - Tools for Experiment and Theory

HELAS and MadGraph with goldstinos

K. Mawatari[1,a], **Y. Takaesu**[2,b]

[1]Theoretische Natuurkunde and IIHE/ELEM, Vrije Universiteit Brussel, and International Solvay Institutes, Pleinlaan 2, 1050 Brussels, Belgium
[2]KEK Theory Center, and Sokendai, Tsukuba 305-0801, Japan

Received: 21 January 2011 / Revised: 27 March 2011 / Published online: 9 June 2011

Abstract Fortran subroutines to calculate helicity amplitudes with goldstinos, which appear as the longitudinal modes of massive gravitinos in high energy processes, are added to the HELAS (HELicity Amplitude Subroutines) library. They are coded in such a way that arbitrary amplitudes with external goldstinos can be generated automatically by MadGraph, after slight modifications. All the codes have been tested carefully by making use of the goldstino equivalence theorem and the gauge invariance of the helicity amplitudes. Hadronic total cross sections for associated gravitino productions with a gluino and a squark are also presented.

1 Introduction

Goldstinos are Goldstone fermions, massless spin-1/2 particles, associated with spontaneous supersymmetry (SUSY) breaking, and appear as the helicity $\pm 1/2$ states of massive gravitinos via the super-Higgs mechanism in local supersymmetric extensions to the Standard Model (SM). While the interactions of the helicity $\pm 3/2$ components of the gravitino are suppressed by the Planck scale, those of the helicity $\pm 1/2$ components are suppressed by the SUSY breaking scale and can be important even for collider phenomenology in low-scale SUSY breaking scenarios, e.g., gauge-mediated SUSY breaking [1].

In the recent paper [2] K. Hagiwara and the authors introduced new HELAS subroutines [3, 4] to calculate helicity amplitudes with massive spin-3/2 gravitinos. They are coded in such a way that arbitrary amplitudes with external gravitinos can be generated automatically by MadGraph [5, 6].

In this paper, taking into account high energy processes with the center-of-mass (CM) energy $\sqrt{s} \gg m_{3/2}$, we present new HELAS subroutines for goldstino interactions based on the effective Lagrangian below, and implement them into MadGraph/MadEvent (MG/ME) v4 [5–8], as an alternative to the code for gravitinos [2].[1] As we will see later, in the high energy limit, the new code for goldstinos agrees with the code for gravitinos with the correction of order $m_{3/2}/\sqrt{s}$ due to the goldstino equivalence theorem. The new code could be useful especially for collider phenomenology, where the goldstino limit is good approximation for most of the cases. Practically, calculations of helicity-summed amplitude squared for goldstino processes are faster than those for gravitino roughly by a factor of four due to the number of the helicity states and the simpler structures of the HELAS subroutines. We also note that the goldstino code can be applied to models such as broken global SUSY and goldstini [9].

The effective interaction Lagrangian for a goldstino in non-derivative form is [10–12]

$$\begin{aligned}\mathcal{L}_{\rm int} = {} & \frac{i(m^2_{\phi^i_{L/R}} - m^2_{f^i})}{\sqrt{3}\,\overline{M}_{\rm Pl} m_{3/2}} \big[\bar{\psi} P_L f^i (\phi^i_L)^* - \bar{f}^i P_R \psi \phi^i_L \\ & - \bar{\psi} P_R f^i (\phi^i_R)^* + \bar{f}^i P_L \psi \phi^i_R\big] \\ & - \frac{m_\lambda}{4\sqrt{6}\,\overline{M}_{\rm Pl} m_{3/2}} \bar{\psi}\big[\gamma^\mu, \gamma^\nu\big]\lambda^{(\alpha)a} F^{(\alpha)a}_{\mu\nu} \\ & + \frac{i g_\alpha m_\lambda}{\sqrt{6}\,\overline{M}_{\rm Pl} m_{3/2}} \bar{\psi}\gamma_5 \lambda^{(\alpha)a} \phi^{i*} T^{(\alpha)a}_{ij} \phi^j \end{aligned} \tag{1}$$

with the reduced Planck mass $\overline{M}_{\rm Pl} \equiv M_{\rm Pl}/\sqrt{8\pi} \sim 2.4 \times 10^{18}$ GeV and the gravitino mass $m_{3/2}$. ψ is the Majorana-spinor goldstino field, f^i and ϕ^i are spinor and scalar fields in the same chiral supermultiplet, and $P_{R/L} = \frac{1}{2}(1 \pm \gamma_5)$ are the chiral-projection operators. $T^{(\alpha=3,2,1)a}$ are the $SU(3)_C$

[a] e-mail: kentarou.mawatari@vub.ac.be
[b] e-mail: takaesu@post.kek.jp

[1]The Fortran code for simulations of the goldstinos/gravitinos is available at the KEK HELAS/MadGraph/MadEvent Home Page, http://madgraph.kek.jp/KEK/.

$(a = 1, \ldots, 8)$, $SU(2)_L$ $(a = 1, 2, 3)$ and $U(1)_Y$ generators, respectively, and $g_{\alpha=3,2,1}$ are the corresponding gauge couplings. The field-strength tensors for each gauge group are

$$F^{(3)a}_{\mu\nu} = \partial_\mu A^a_\nu - \partial_\nu A^a_\mu - g_3 f_3^{abc} A^b_\mu A^c_\nu, \tag{2}$$

$$F^{(2)a}_{\mu\nu} = \partial_\mu W^a_\nu - \partial_\nu W^a_\mu - g_2 f_2^{abc} W^b_\mu W^c_\nu, \tag{3}$$

$$F^{(1)a}_{\mu\nu} = \partial_\mu B_\nu - \partial_\nu B_\mu, \tag{4}$$

and the corresponding gauginos $\lambda^{(\alpha=3,2,1)a}$ are gluinos $(\tilde{g}^a)$, winos $(\tilde{W}^a)$ and bino $(\tilde{B})$, respectively.

The equivalence of the non-derivative form in (1) and the derivative form which is obtained by the replacement of the gravitino field $\psi_\mu \sim \sqrt{2/3}\partial_\mu \psi / m_{3/2}$ in the gravitino interaction Lagrangian (see, e.g. Eq. (2) in [2]) has been proved in [11]. The following features of the interaction Lagrangian (1) are worth noting: (i) The ψ-f-ϕ-A_μ vertex is absent, while a new quartic vertex, ψ-λ-ϕ-ϕ, exists. (ii) The couplings are proportional to the mass splitting inside the supermultiplet, $m^2_{\phi^i} - m^2_{f^i}$ and m_λ, and inversely proportional to the SUSY-breaking vacuum expectation value through the gravitino mass

$$m_{3/2} = \langle F \rangle / \sqrt{3}\, \overline{M}_{\rm Pl}. \tag{5}$$

The paper is organized as follows: In Sect. 2 we test our code by making use of the goldstino equivalence theorem, and in Sect. 3 we give hadronic total cross sections of associated gravitino productions with a gluino and a squark as sample numerical results. Section 4 presents our brief summary. In Appendix A we give the new HELAS subroutines for goldstinos, and in Appendix B we describe how to implement the amplitudes into MG.

2 Checking the goldstino–gravitino equivalence

In this section, we check the new HELAS subroutines and the modified MG for goldstinos by using the goldstino equivalence theorem. As mentioned in Introduction, goldstinos appear as the longitudinal modes of massive gravitinos and their interactions become dominant over the transverse modes in high-energy processes. By using the MG/ME package with gravitinos [2], we test an agreement between the goldstino amplitudes and the gravitino amplitudes in the high-energy limit.

We consider the goldstino production processes associated with a squark

$$q + g \to \tilde{q} + \tilde{G} \quad \text{and} \quad \bar{q} + g \to \bar{\tilde{q}} + \tilde{G}, \tag{6}$$

which involves the ψ-f-ϕ vertex as well as ψ-λ-A_μ, and with a gluino for the gg initial state

$$g + g \to \tilde{g} + \tilde{G}, \tag{7}$$

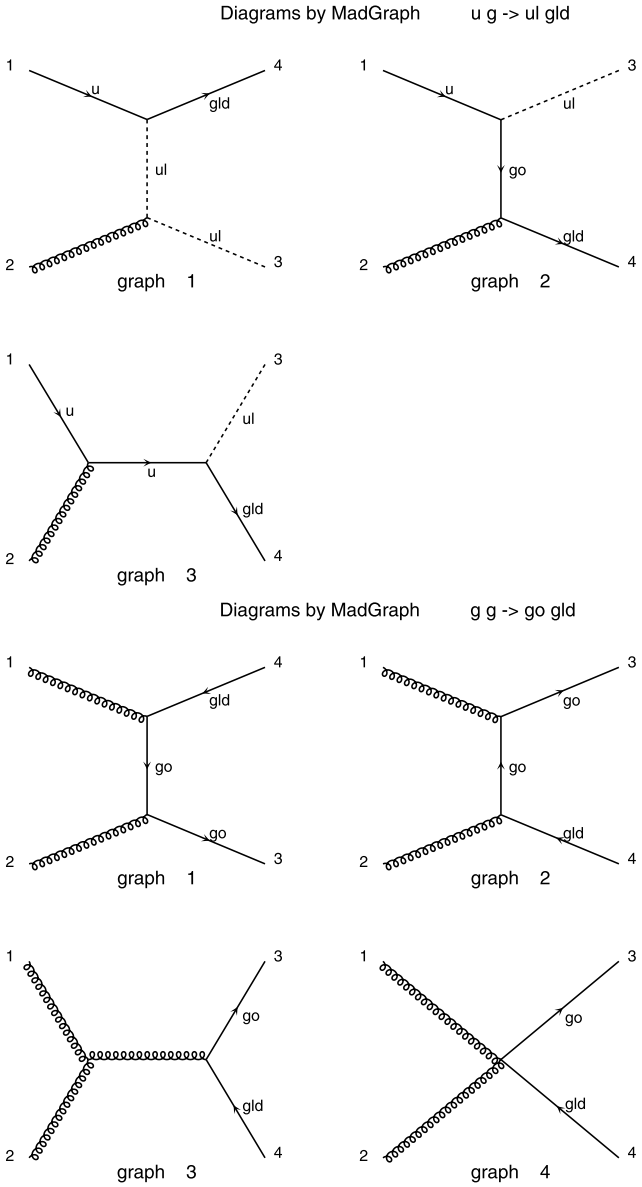

Fig. 1 Feynman diagrams for associated goldstino productions with a squark, $qg \to \tilde{q}\tilde{G}$ (*top*), and with a gluino, $gg \to \tilde{g}\tilde{G}$ (*bottom*), generated by MadGraph. ul, go, and gld denote a sup, a gluino, and a goldstino, respectively

which involves the ψ-λ-A_μ and ψ-λ-A_μ-A_ν vertices. The Feynman diagrams shown in Fig. 1 and the corresponding helicity amplitudes are generated automatically by the modified MG. The details of the HELAS subroutines for goldstinos and those implementation to MG are presented in appendices. We note that, in the gravitino case, a diagram with the quartic ψ_μ-f-ϕ-A_ν vertex exists for the squark-gravitino production.

Figure 2 shows squared matrix elements of the above two processes, $qg \to \tilde{q}\tilde{G}$ (a) and $gg \to \tilde{g}\tilde{G}$ (b), at the partonic CM energy $\sqrt{\hat{s}} = 2$ TeV and at the partonic scattering angle $\cos\hat{\theta} = 0.5$ as a function of the gravitino mass $(m_{3/2})$. The

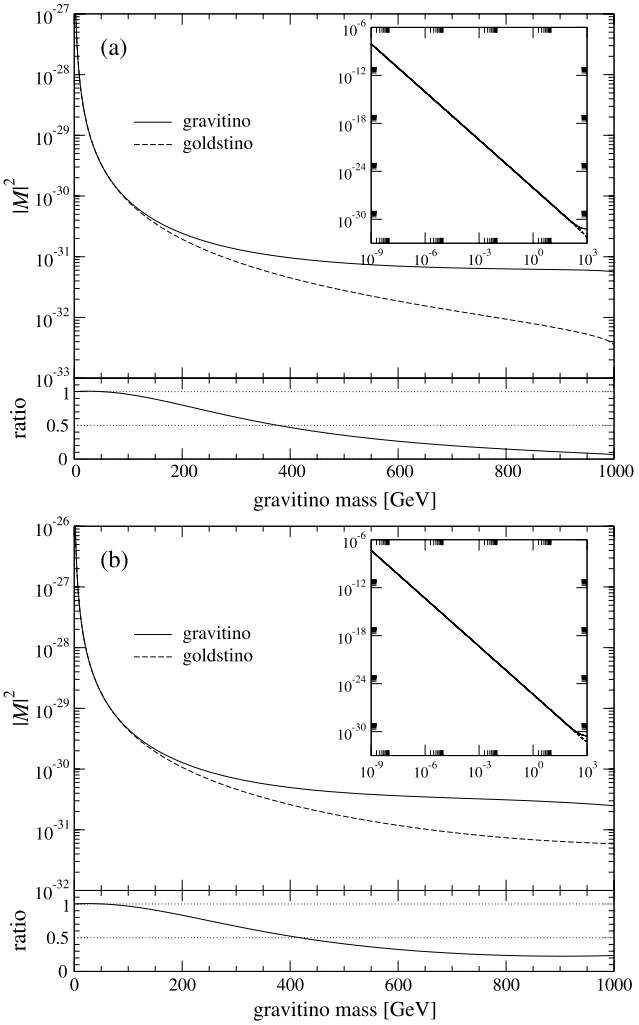

Fig. 2 Squared matrix elements of gravitino (*solid*) and goldstino (*dashed*) productions associated with a squark, $qg \to \tilde{q}\tilde{G}$ (**a**), and with a gluino for the gg initial state, $gg \to \tilde{g}\tilde{G}$ (**b**), at $\sqrt{\hat{s}} = 2$ TeV and $\cos\hat{\theta} = 0.5$ as a function of the gravitino mass, where the squark and gluino masses are fixed at 1 TeV. The ratios of the squared matrix elements are also shown

squark and gluino masses are fixed at 1 TeV. In the region of the small gravitino mass, $m_{3/2}/\sqrt{\hat{s}} < 0.05$, or in the high energy region $\sqrt{\hat{s}} \gg m_{3/2}$, the ratio of the squared matrix elements, $|M_{\text{goldstino}}|^2/|M_{\text{gravitino}}|^2$, is nearly unity, that is, both amplitudes agree well each other. We note that the squared matrix elements for the associated gravitino productions are proportional to $m_{3/2}^{-2}$ as clearly seen in the log–log plot in Fig. 2. Associated productions of gravitino and gluino for the $q\bar{q}$ initial state

$$q + \bar{q} \to \tilde{g} + \tilde{G}, \tag{8}$$

which involves the ψ-f-ϕ and ψ-λ-A_μ vertices, can be also tested, as well as the above processes with an extra parton and crossed processes.

Before turning to sample results, we also note that, in addition to the goldstino-gravitino equivalence test, the code was checked carefully by comparing with the analytical squared matrix elements of Eqs. (3), (5) and (7) in Ref. [13] for the above three partonic processes. The hadronic total cross sections at the SUSY benchmark points SPS7 and SPS8 in Figs. 8 and 11 in Ref. [13] can also be reproduced with the help of ME [7, 8]. The test by using the gauge invariance of the amplitudes is also mentioned in Appendix A.4.

3 Sample results

In this section, we present some sample numerical results, using the new HELAS subroutines, which are presented in Appendix A, and the modified MG, which is described in Appendix B.

In gauge-mediated SUSY breaking scenarios, the gravitino is often the lightest supersymmetric particle (LSP), and its phenomenology depends on what the next-to-lightest supersymmetric particle (NLSP) is. While the lightest neutralino and the lighter stau are often the NLSP in minimal models of gauge mediation, gluinos can also be the NLSP, e.g., in split SUSY models and general gauge mediation models; see review papers [1, 14] and references therein.

If gluinos are the NLSP and light enough, those productions can be explored in the early LHC data as well as in the Tevatron, and several studies have been performed for hadroproductions of a gravitino with a gluino (or a squark) [13, 15–17], which lead to characteristic signals of monojet plus missing energy when a produced gluino (squark) promptly decays into a gluon (quark) and a LSP gravitino. We consider such scenarios for sample results of our code.

Figure 3 presents total cross sections of each subprocess of associated gravitino productions with a gluino,

$$p\bar{p}/pp \to \tilde{g}\tilde{G}, \tag{9}$$

at the Tevatron-1.96 TeV/LHC-7 TeV for the gravitino mass $m_{3/2} = 10^{-13}$ GeV as a function of the gluino mass. The masses of the left-handed and right-handed squarks, which appear in the t- and u-channel propagators, are fixed at 1.5 TeV (dashed lines) and $2m_{\tilde{g}}$ (dotted lines) for the $q\bar{q}$ subprocesses. The cross sections of associated productions with a squark,

$$p\bar{p}/pp \to \tilde{q}\tilde{G} \text{ and } \bar{\tilde{q}}\tilde{G}, \tag{10}$$

as a function of the squark mass are also shown in Fig. 4 for reference, where the productions of the left-handed and right-handed squarks are summed and their masses

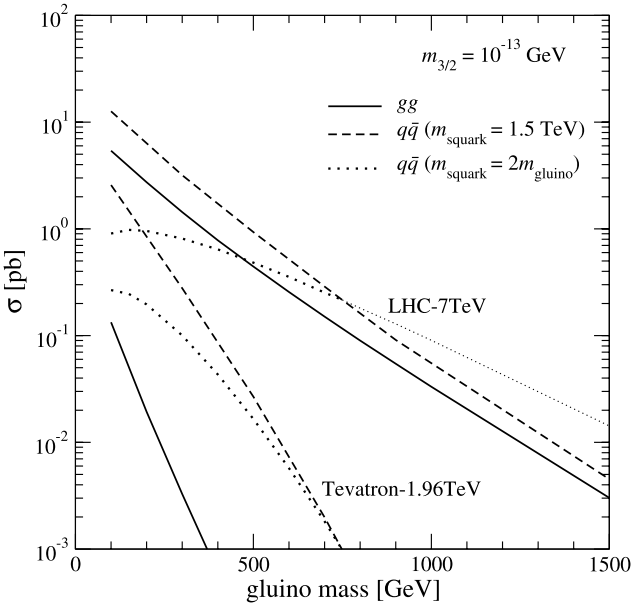

Fig. 3 Total cross sections of each subprocess of associated gravitino productions with a gluino, $p\bar{p}/pp \to \tilde{g}\tilde{G}$, at the Tevatron-1.96 TeV/LHC-7 TeV for $m_{3/2} = 10^{-13}$ GeV as a function of the gluino mass. The squark masses are fixed at 1.5 TeV (*dashed*) and $2m_{\tilde{g}}$ (*dotted*) for the $q\bar{q}$ subprocesses, where the cross section in the $\Gamma_{\tilde{q}\to q\tilde{G}} > m_{\tilde{q}}/2$ region is shown with a thin *dotted line*

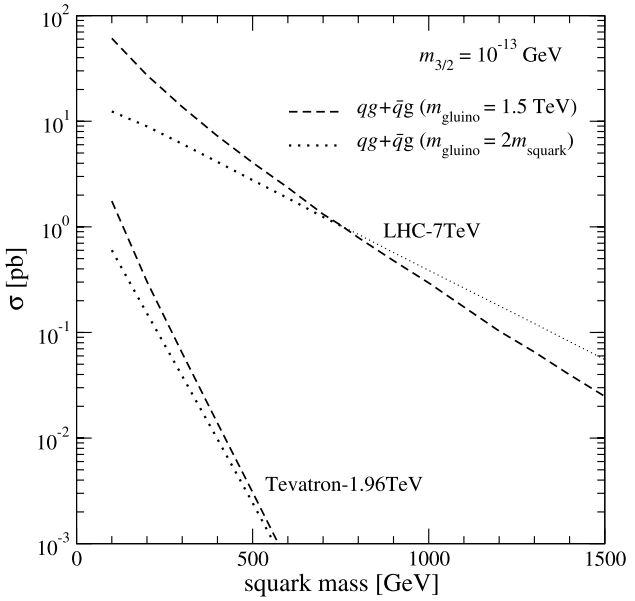

Fig. 4 Total cross sections of associated gravitino productions with a squark, $p\bar{p}/pp \to \tilde{q}\tilde{G}$, at the Tevatron-1.96 TeV/LHC-7 TeV for $m_{3/2} = 10^{-13}$ GeV as a function of the squark mass. The gluino masses are fixed at 1.5 TeV (*dashed*) and $2m_{\tilde{q}}$ (*dotted*), where the cross section in the $\Gamma_{\tilde{g}\to g\tilde{G}} > m_{\tilde{g}}/2$ region is shown with a *thin dotted line*

are taken to be same. The gluino mass is fixed at 1.5 TeV (dashed lines) and $2m_{\tilde{q}}$ (dotted lines). The CTEQ6L1 parton distribution functions [18] are employed, and the renormalization and factorization scales are fixed at the average mass of the final state particles, $\mu_R = \mu_F = (m_{\tilde{g},\tilde{q}} + m_{3/2})/2 \sim m_{\tilde{g},\tilde{q}}/2$. The cross section in the partial width $\Gamma_{\tilde{q}(\tilde{g})\to q(g)\tilde{G}} > m_{\tilde{q}(\tilde{g})}/2$ region is shown with a thin dotted line in Figs. 3, 4, which will be discussed later.

The major features of the production cross sections are following:

- The cross sections of all the subprocesses scale with $m_{3/2}^{-2}$, that is, lighter gravitinos enhance the monojet signals, which can be interpreted as the direct lower bound for the gravitino mass.[2] Note that, on the other hand, the dijet signals which are produced through gluino-pair productions do not depend on the gravitino mass.
- The gluino–gravitino associated productions through the gg initial state depend only on the gluino mass once the gravitino mass is fixed, while the $q\bar{q}$-initiated production cross section depends not only on the gluino mass but also on the t- and u-channel-exchanged squark masses. It should be noted that those contributions are not decoupled in the large squark mass limit, and the heavier squark exchange increases the cross section since the goldstino–quark–squark couplings are proportional to the squark mass squared. Therefore, for heavy squark cases, the cross section of the $q\bar{q}$ channel can be larger than that of the gg channel even for the pp collider, LHC.
- Similar to the gluino productions through the $q\bar{q}$ subprocesses, the squark–gravitino associated productions, which are only produced through the qg subprocesses, involve the t-channel gluino exchange diagram as well as the squark exchange one (see Fig. 1 (top)), and the heavy gluino increases the cross section.

Finally, it is worth noting that the partial width of a gluino (squark) decay into a gluon (massless quark) and a gravitino is given by

$$\Gamma_{\tilde{g}(\tilde{q})\to g(q)\tilde{G}} = \frac{m_{\tilde{g}(\tilde{q})}^5}{48\pi \overline{M}_{\rm Pl}^2 m_{3/2}^2}. \tag{11}$$

Therefore, as the gravitino mass becomes small and/or the gluino (squark) mass becomes large, the partial width rapidly grows. For instance, in the $m_{3/2} = 10^{-13}$ GeV case, $\Gamma = 1.12 \times 10^{-3}$ GeV for $m_{\tilde{g}(\tilde{q})} = 100$ GeV, while $\Gamma = 850$ GeV for $m_{\tilde{g}(\tilde{q})} = 1.5$ TeV. When the width becomes a significant fraction of the mass, the goldstino coupling becomes strong and the perturbative calculations are unreliable. Thin dotted lines in Figs. 3 and 4 show such parameter

[2] The current lower bound from the Tevatron with the integrated luminosity of 87 pb^{-1} is about 10^{-14} GeV [19], where all the SUSY particles except gravitino are assumed to be too heavy to be produced on-shell [20].

regions. Moreover, the decay branching ratios depend on the entire SUSY mass spectrum; see, e.g., Ref. [13]. Therefore, the comprehensive analyses are necessary for the collider signatures such as monojet plus missing energy.

4 Summary

In this paper, we have added new HELAS subroutines to calculate helicity amplitudes with goldstinos, which appear as the longitudinal modes of massive gravitinos in high energy processes, into the HELAS library. They are coded in such a way that arbitrary amplitudes with external goldstinos can be generated automatically by MadGraph, after slight modifications. All the codes have been tested carefully by making use of the goldstino equivalence theorem and the gauge invariance of the helicity amplitudes. Total cross sections of associated gravitino productions with a gluino and a squark are also presented for the Tevatron and the LHC as sample results.

Acknowledgements We wish to thank Kaoru Hagiwara and Alberto Mariotti for valuable discussions and comments and Junichi Kanzaki for putting our code on the web. We also would like to thank Tilman Plehn and the members of the ITP, Uni. Heidelberg for their warm hospitality, where part of this work has been done. The work presented here has been in part supported by the Concerted Research action "Supersymmetric Models and their Signatures at the Large Hadron Collider" of the Vrije Universiteit Brussel, by the IISN "MadGraph" convention 4.4511.10, by the Belgian Federal Science Policy Office through the Interuniversity Attraction Pole IAP VI/11, and by the Grant-in-Aid for Scientific Research (No. 20340064) from the Japan Society for the Promotion of Science. Y.T. was also supported in part by Institutional Program for Young Researcher Overseas Visits.

Appendix A: HELAS subroutines for goldstinos

In this appendix, we list the contents of all the new HELAS subroutines that are needed to evaluate processes with an external goldstino based on the effective Lagrangian of (1).

In Appendixes A.1 to A.3, we explain vertex subroutines listed in Table 1, which compute interactions among a goldstino with SM and SUSY particles. Those subroutines which we do not present in this paper are a FFSS type vertex, the last term in (1). This contributes to some phenomenology in cosmology, e.g., the goldstino emission rate through $\tilde{q}\tilde{\bar{q}} \to \tilde{g}\tilde{G}$ and $\tilde{q}\tilde{g} \to \tilde{q}\tilde{G}$ [11], but it is mostly irrelevant in collider signatures. In Appendix A.4 we briefly mention a test of our new subroutines by making use of the gauge invariance.

Table 1 List of the new vertex subroutines in HELAS system

Vertex	Inputs	Output	Subroutine
FFS	FFS	Amplitude	IORSGX, IROSGX
	FS	F	FSORGX, FSIRGX
	FF	S	HIORGX, HIROGX
FFV	FFV	Amplitude	IORVGX, IROVGX
	FV	F	FVORGX, FVIRGX
	FF	V	JIORGX, JIROGX
FFVV	FFVV	Amplitude	IORVVG, IROVVG
	FVV	F	FVVORG, FVVIRG
	FFV	V	JVIORG, JVIROG

Before turning to vertex subroutines, we note that the existing subroutines for flowing-in (IXXXXX) and -out (OXXXXX) spinor wavefunctions can be applied for a goldstino without any modification since it is just a spin-1/2 particle.

A.1 FFS vertex

The FFS vertices involving a goldstino are obtained from the interaction Lagrangian among a fermion (f), a goldstino (ψ) and a scalar boson (S):

$$\mathcal{L}_{\mathtt{FFS}} = \bar{\psi}\big(\mathtt{GC(1)}P_L + \mathtt{GC(2)}P_R\big) f S^* + \text{h.c.} \tag{A.1}$$

with the chiral-projection operator $P_{R/L} = \frac{1}{2}(1 \pm \gamma_5)$. The interaction vertices are exactly same as those in the present HELAS library, i.e., the Yukawa-type vertex. Therefore, we simply reuse the existing IOSXXX, FSOXXX and HIOXXX subroutines for IORSGX, FSORGX and HIORGX, respectively, while IROSGX, FSIRGX and HIROGX need coupling modification due to the Hermitian conjugate as

$$\begin{aligned} \mathtt{GC'(1)} &= \big(\mathtt{GC(2)}\big)^*, \\ \mathtt{GC'(2)} &= \big(\mathtt{GC(1)}\big)^*, \end{aligned} \tag{A.2}$$

in order to reuse IOSXXX, FSIXXX and HIOXXX, respectively. The correspondence between the new HELAS subroutines and the existing ones are shown in Table 2; see also the HELAS manual [3, 4] for details of these subroutines.

GC(1) and GC(2) are the relevant left- and right-coupling constants. For instance, in the case of the quark-goldstino-squark interaction without squark mixing, q-$\tilde{G}$-$\tilde{q}_\alpha$, those couplings read

$$\begin{cases} \mathtt{GC(1)} = \mathtt{GFFSL(1)} = \mathtt{GFFS} \\ \mathtt{GC(2)} = \mathtt{GFFSL(2)} = 0 \end{cases} \quad \text{for } \alpha = L, \tag{A.3}$$

$$\begin{cases} \mathtt{GC(1)} = \mathtt{GFFSR(1)} = 0 \\ \mathtt{GC(2)} = \mathtt{GFFSR(2)} = -\mathtt{GFFS} \end{cases} \quad \text{for } \alpha = R, \tag{A.4}$$

Table 2 Reference HELAS subroutines in the present HELAS library [3, 4] to the new ones

Vertex	New subroutine	Reference subroutine
FFS	IORSGX, IROSGX	IOSXXX
	FSORGX	FSOXXX
	FSIRGX	FSIXXX
	HIORGX, HIROGX	HIOXXX

with

$$\texttt{GFFS} = im_{\tilde{q}_\alpha}^2/\sqrt{3}\,\overline{M}_{\rm Pl} m_{3/2} \tag{A.5}$$

in the quark massless limit. We note that, in the HELAS convention, the factors of i in the goldstino coupling constants are necessary to give a correct phase between the amplitudes which involve particles in minimal supersymmetric standard model (MSSM) plus goldstinos.

A.2 FFV vertex

The FFV vertices involving a goldstino are obtained from the interaction Lagrangian among a fermion, a goldstino fermion and a vector boson (V^μ):

$$\mathcal{L}_{\rm FFV} = -i\bar{\psi}\big[\gamma^\mu,\gamma^\nu\big]\big(\texttt{GC(1)}P_L + \texttt{GC(2)}P_R\big) f\partial_\mu V_\nu^* + \text{h.c.} \tag{A.6}$$

Although both a goldstino and a gaugino are Majorana particles in most cases, the Hermitian conjugate term is necessary for MG; practically, either the first or second term is used in calculations of amplitudes with the coupling constant

$$\texttt{GC(1)} = \texttt{GC(2)} = \texttt{GFFV} = -im_f/2\sqrt{6}\,\overline{M}_{\rm Pl} m_{3/2} \tag{A.7}$$

in units of GeV^{-1}, where m_f is the gaugino mass.

We note that the input and output parameters of the subroutines for the FFV goldstino vertices are completely same as those of the existing FFV-type subroutines, though the vertex structure computed in the subroutines is different.

A.2.1 IORVGX

This subroutine computes an amplitude of the FFV goldstino vertex from wavefunctions of a flowing-in fermion, a flowing-out goldstino and a vector boson, and should be called as

```
CALL IORVGX(FI,FO,VC,GC,VERTEX).
```

The inputs FI(6) and FO(6) are complex six-dimensional arrays which consist of the wavefunction and the four-momentum of the flowing-In and -Out Fermion as

$$p_{\rm I}^\mu = \big(\Re e\,\texttt{FI(5)}, \Re e\,\texttt{FI(6)}, \Im m\,\texttt{FI(6)}, \Im m\,\texttt{FI(5)}\big),$$

$$p_{\rm O}^\mu = \big(\Re e\,\texttt{FO(5)}, \Re e\,\texttt{FO(6)}, \Im m\,\texttt{FO(6)}, \Im m\,\texttt{FO(5)}\big),$$

respectively. VC(6) is a complex six-dimensional array which contains the Vector boson wavefunction and its momentum as

$$q^\mu = \big(\Re e\,\texttt{VC(5)}, \Re e\,\texttt{VC(6)}, \Im m\,\texttt{VC(6)}, \Im m\,\texttt{VC(5)}\big).$$

The input GC(2) is the coupling constant in (A.7). The output VERTEX is a complex number:

$$\texttt{VERTEX} = \texttt{(FO)}[\not{q}, \not{V}]\big(\texttt{GC(1)}P_L + \texttt{GC(2)}P_R\big)\texttt{(FI)}, \tag{A.8}$$

where we use the notations

$$\texttt{(FI)} = \begin{pmatrix} \texttt{FI(1)} \\ \texttt{FI(2)} \\ \texttt{FI(3)} \\ \texttt{FI(4)} \end{pmatrix}, \tag{A.9}$$

$$\texttt{(FO)} = \big(\texttt{FO(1)}, \texttt{FO(2)}, \texttt{FO(3)}, \texttt{FO(4)}\big), \tag{A.10}$$

$$V^\mu = \texttt{VC}(\mu+1). \tag{A.11}$$

A.2.2 FVORGX

This subroutine computes an off-shell fermion wavefunction made from the interaction of a vector boson and a flowing-out goldstino by the FFV goldstino vertex, and should be called as

```
CALL FVORGX(FO,VC,GC,FMASS,
            FWIDTH,FVORG),
```

where the inputs FMASS and FWIDTH are the mass and the width of the off-shell fermion, m_F and Γ_F. The output FVORG(6) is a complex six-dimensional array and gives the off-shell fermion wavefunction multiplied by the fermion propagator and its momentum as

$$\texttt{(FVORG)} = \texttt{(FO)}[\not{q}, \not{V}]\big(i\texttt{GC(1)}P_L + i\texttt{GC(2)}P_R\big) \times \frac{i(\not{p}+m_F)}{p^2 - m_F^2 + im_F\Gamma_F}, \tag{A.12}$$

and

$$\texttt{FVORG(5)} = \texttt{FO(5)} + \texttt{VC(5)}, \tag{A.13}$$

$$\texttt{FVORG(6)} = \texttt{FO(5)} + \texttt{VC(6)}, \tag{A.14}$$

where we use the notation

(FVORG)

$$= \big(\texttt{FVORG(1)}, \texttt{FVORG(2)}, \texttt{FVORG(3)}, \texttt{FVORG(4)}\big),$$

and the momentum p is

$$p^\mu = \big(\Re e\,\texttt{FVORG(5)}, \Re e\,\texttt{FVORG(6)}, \Im m\,\texttt{FVORG(6)}, \Im m\,\texttt{FVORG(5)}\big).$$

A.2.3 JIORGX

This subroutine computes an off-shell vector current made from the interaction of a flowing-in fermion and a flowing-out goldstino by the FFV goldstino vertex, and should be called as

```
CALL JIORGX(FI, FO, GC, VMASS,
            VWIDTH, JIORG),
```

where the inputs VMASS and VWIDTH are the mass and the width of the vector boson, m_V and Γ_V. The output JIORG(6) is a complex six-dimensional array and gives the off-shell vector current multiplied by the vector boson propagator and its momentum as

$$\begin{aligned}&\texttt{JIORG}(\mu+1)\\ &= \frac{i}{q^2 - m_V^2 + i m_V \Gamma_V}\left(-g^{\mu\nu} + \frac{q^\mu q^\nu}{m_V^2}\right)\\ &\quad\times (\texttt{FO})[\not{q}, \gamma_\nu]\big(i\texttt{GC(1)}P_L + i\texttt{GC(2)}P_R\big)(\texttt{FI})\end{aligned} \tag{A.15}$$

for the massive vector boson, or

$$\begin{aligned}&\texttt{JIORG}(\mu+1)\\ &= \frac{-i}{q^2}(\texttt{FO})\big[\not{q}, \gamma^\mu\big]\big(i\texttt{GC(1)}P_L + i\texttt{GC(2)}P_R\big)(\texttt{FI})\end{aligned} \tag{A.16}$$

for the massless vector boson, and

$$\texttt{JIORG(5)} = -\texttt{FI(5)} + \texttt{FO(5)},$$

$$\texttt{JIORG(6)} = -\texttt{FI(6)} + \texttt{FO(6)}.$$

Here, q is the momentum of the off-shell vector boson,

$$q^\mu = \big(\Re e\,\texttt{JIORG(5)}, \Re e\,\texttt{JIORG(6)}, \Im m\,\texttt{JIORG(6)}, \Im m\,\texttt{JIORG(5)}\big).$$

Note that we use the unitary gauge for the massive vector boson propagator and the Feynman gauge for the massless one, according to the HELAS convention [3, 4].

A.2.4 IROVGX

This is essentially the same subroutine as IORVGX but modifies the input coupling GC as in (A.3) since this computes the Hermitian conjugate vertex of IORVGX.

A.2.5 FVIRGX

This subroutine computes an off-shell fermion wavefunction made from the interaction of a vector boson and a flowing-in goldstino by the FFV goldstino vertex, and should be called as

```
CALL FVIRGX(FI, VC, GC, FMASS,
            FWIDTH, FVIRG).
```

What we compute here is

$$\begin{aligned}(\texttt{FVIRG}) &= \frac{i(\not{p} + m_F)}{p^2 - m_F^2 + i m_F \Gamma_F}\\ &\quad\times \big(i\texttt{GC(1)}^* P_R + i\texttt{GC(2)}^* P_L\big)[\not{q}, \not{V}](\texttt{FI}),\end{aligned}$$

and

$$\texttt{FVIRG(5)} = \texttt{FI(5)} - \texttt{VC(5)}, \tag{A.17}$$

$$\texttt{FVIRG(6)} = \texttt{FI(6)} - \texttt{VC(6)}, \tag{A.18}$$

where we use the notation

$$(\texttt{FVIRG}) = \begin{pmatrix}\texttt{FVIRG(1)}\\ \texttt{FVIRG(2)}\\ \texttt{FVIRG(3)}\\ \texttt{FVIRG(4)}\end{pmatrix}, \tag{A.19}$$

and the momentum p is

$$p^\mu = \big(\Re e\,\texttt{FVIRG(5)}, \Re e\,\texttt{FVIRG(6)}, \Im m\,\texttt{FVIRG(6)}, \Im m\,\texttt{FVIRG(5)}\big).$$

A.2.6 JIROGX

This is essentially the same subroutine as JIORGX but modifies the input coupling GC as in (A.3) since this computes the Hermitian conjugate vertex of JIORGX.

A.3 FFVV vertex

The FFVV vertices involving a goldstino are obtained from the interaction Lagrangian among a fermion, a goldstino and two vector bosons:

$$\begin{aligned}\mathcal{L}_{\texttt{FFVV}} &= i f^{abc}\bar{\psi}\big[\gamma^\mu, \gamma^\nu\big]\big(\texttt{GC(1)}P_L\\ &\quad + \texttt{GC(2)}P_R\big) f^a V_\mu^b V_\nu^c + \text{h.c.}\end{aligned} \tag{A.20}$$

with the structure constant f^{abc}, which can be handled by the MG automatically. As in the FFV vertex case, we need the Hermitian conjugate term although a goldstino and a gaugino are Majorana particles in most cases. The coupling constant GC is the product of the FFV goldstino coupling constant and the gauge coupling constant of the involving gauge

boson. For instance, in the case of the goldstino-gluino-gluon-gluon interaction, $\tilde{G}$-$\tilde{g}$-g-g, those couplings are

$$\mathtt{GC(1)} = \mathtt{GC(2)} = \mathtt{GFFV} * \mathtt{Gs} = -im_f g_s/2\sqrt{6}\,\overline{M}_{\mathrm{Pl}} m_{3/2} \tag{A.21}$$

in units of GeV^{-1}, where $\mathtt{Gs} = g_s$ is the strong coupling constant.

A.3.1 IORVVG

This subroutine computes an amplitude of the FFVV goldstino vertex from a flowing-in fermion, a flowing-out goldstino and two vector bosons, and should be called as

```
CALL IORVVG(FI,FO,VA,VB,GC,VERTEX).
```

What we compute here is

$$\mathtt{VERTEX} = (\mathtt{FO})\big[\not{V}^a, \not{V}^b\big]\big(\mathtt{GC(1)}P_L + \mathtt{GC(2)}P_R\big)(\mathtt{FI}), \tag{A.22}$$

where we use the notations

$$V^{a,\mu} = \mathtt{VA}(\mu+1), \tag{A.23}$$

$$V^{b,\mu} = \mathtt{VB}(\mu+1). \tag{A.24}$$

A.3.2 FVVORG

This subroutine computes an off-shell fermion wavefunction made from the interaction of two vector bosons and a flowing-out goldstino by the FFVV goldstino vertex, and should be called as

```
CALL FVVORG(FO, VA, VB, GC, FMASS,
            FWIDTH, FVVORG).
```

What we compute here is

$$(\mathtt{FVVORG}) = (\mathtt{FO})\big[\not{V}^a, \not{V}^b\big]\big(i\mathtt{GC(1)}P_L + i\mathtt{GC(2)}P_R\big) \times \frac{i(\not{p}+m_F)}{p^2 - m_F^2 + im_F\Gamma_F}, \tag{A.25}$$

and

$$\mathtt{FVVORG(5)} = \mathtt{FO(5)} + \mathtt{VA(5)} + \mathtt{VB(5)}, \tag{A.26}$$

$$\mathtt{FVVORG(6)} = \mathtt{FO(6)} + \mathtt{VA(6)} + \mathtt{VB(6)}, \tag{A.27}$$

where we use the notation

$$(\mathtt{FVVORG}) = \big(\mathtt{FVVORG(1)}, \mathtt{FVVORG(2)}, \mathtt{FVVORG(3)}, \mathtt{FVVORG(4)}\big), \tag{A.28}$$

and the momentum p is

$$p^\mu = \big(\Re e\,\mathtt{FVVORG(5)}, \Re e\,\mathtt{FVVORG(6)}, \Im m\,\mathtt{FVVORG(6)}, \Im m\,\mathtt{FVVORG(5)}\big).$$

A.3.3 JVIORG

This subroutine computes an off-shell vector current made from the interaction of a vector boson, a flowing-in fermion and a flowing-out goldstino by the FFVV goldstino vertex, and should be called as

```
CALL JVIORG(FI, FO, VC, GC, VMASS,
            VWIDTH, JVIORG).
```

What we compute here is

$$\mathtt{JVIORG}(\mu+1) = \frac{i}{q^2 - m_V^2 + im_V\Gamma_V}\left(-g^{\mu\nu} + \frac{q^\mu q^\nu}{m_V^2}\right) \times (\mathtt{FO})[\gamma_\nu, \not{V}]\big(i\mathtt{GC(1)}P_L + i\mathtt{GC(2)}P_R\big)(\mathtt{FI}) \tag{A.29}$$

for the massive vector boson, or

$$\mathtt{JVIORG}(\mu+1) = \frac{-i}{q^2}(\mathtt{FO})\big[\gamma^\mu, \not{V}\big]\big(i\mathtt{GC(1)}P_L + i\mathtt{GC(2)}P_R\big)(\mathtt{FI}) \tag{A.30}$$

for the massless vector boson, and

$$\mathtt{JVIORG(5)} = -\mathtt{FI(5)} + \mathtt{FO(5)} + \mathtt{VC(5)}, \tag{A.31}$$

$$\mathtt{JVIORG(6)} = -\mathtt{FI(6)} + \mathtt{FO(6)} + \mathtt{VC(6)}, \tag{A.32}$$

where momentum q is

$$q^\mu = \big(\Re e\,\mathtt{JVIORG(5)}, \Re e\,\mathtt{JVIORG(6)}, \Im m\,\mathtt{JVIORG(6)}, \Im m\,\mathtt{JVIORG(5)}\big).$$

A.3.4 IROVVG

This is essentially the same subroutine as IORVVG but modifies the input coupling GC as in (A.3) since this computes the Hermitian conjugate vertex of IORVVG.

A.3.5 FVVIRG

This subroutine computes an off-shell fermion wavefunction made from the interaction of two vector bosons and a flowing-in goldstino by the FFVV goldstino vertex, and should be called as

```
CALL FVVIRG(FI, VA, VB, GC, FMASS,
            FWIDTH, FVVIRG).
```

What we compute here is

(FVVIRG)

$$= \frac{i(\not{p} + m_F)}{p^2 - m_F^2 + i m_F \Gamma_F} \big(i\mathrm{GC}(1)^* P_R + i\mathrm{GC}(2)^* P_L\big)\big[\not{V}^a, \not{V}^b\big](\mathrm{FI}), \tag{A.33}$$

and

$$\mathrm{FVVIRG}(5) = \mathrm{FI}(5) - \mathrm{VA}(5) - \mathrm{VB}(5), \tag{A.34}$$

$$\mathrm{FVVIRG}(6) = \mathrm{FI}(6) - \mathrm{VA}(6) - \mathrm{VB}(6), \tag{A.35}$$

where we use the notation

$$(\mathrm{FVVIRG}) = \begin{pmatrix} \mathrm{FVVIRG}(1) \\ \mathrm{FVVIRG}(2) \\ \mathrm{FVVIRG}(3) \\ \mathrm{FVVIRG}(4) \end{pmatrix}, \tag{A.36}$$

and the momentum p is

$$p^\mu = \big(\Re e\,\mathrm{FVVIRG}(5), \Re e\,\mathrm{FVVIRG}(6), \Im m\,\mathrm{FVVIRG}(6), \Im m\,\mathrm{FVVIRG}(5)\big).$$

A.3.6 JVIROG

This is essentially the same subroutine as JVIORG but modifies the input coupling GC as in (A.3) since this computes the Hermitian conjugate vertex of JVIORG.

A.4 Checking for the new HELAS subroutines

In addition to the goldstino-gravitino equivalence test in Sect. 2, the new HELAS subroutines are tested by using the gauge invariance. Helicity amplitudes involving external gluons are expressed as

$$\mathcal{M}_{\lambda_g} = \epsilon_\mu(p_g, \lambda_g) T^\mu \tag{A.37}$$

by extracting one of the gluon wavefunctions, $\epsilon_\mu(p_g, \lambda_g)$, with a momentum p_g and a helicity λ_g. The identity for the $SU(3)$ gauge invariance

$$p_{g_\mu} T^\mu = 0 \tag{A.38}$$

can be used for checking HELAS subroutines. In particular, we test the invariance of the following processes;

$qg \to \tilde{q}\tilde{G}$ for FFS and FFV subroutines,

$gg \to \tilde{g}\tilde{G}g$ for FFV and FFVV subroutines.

We also test the agreement of the helicity-summed amplitude squared evaluated in arbitrary Lorentz frames.

Table 3 List of the coupling constants for each goldstino vertex involving SUSY QCD particles. All the particles and the coupling constants are written in the MG notation. gld stands for a goldstino, q represents a light quark, and ql/qr is a left/right-handed squark. g and go are a gluon and a gluino, respectively. GC is a coupling constant defined in each subroutine in Appendix A

3-point couplings					GC
FFS	q	gld	ql		GFFSL
	q	gld	qr		GFFSR
FFV	go	gld	g		GFFV
4-point couplings					GC
FFVV	go	gld	g	g	GFFVV = GFFV*Gs

Appendix B: Implementation of goldstinos into MadGraph

In this appendix, we describe how we implement goldstinos and their interactions into MG.

First, using the default mssm model in MG/MEv4 [8], we make our new model directory, mssm_goldstino, where we define a goldstino (particles.dat) and its interactions with SM and SUSY particles (interactions.dat and couplings.f); we show the coupling constants for each goldstino vertex involving SUSY QCD particles in Table 3 as examples.[3] Then we add all the new HELAS subroutines for goldstinos to the HELAS library in MG. Although the present MG can handle spin-1/2 particles, we simply replace spin-3/2 gravitinos in the recent modified MG [2] by goldstinos since the FFV goldstino vertex is non-renormalizable and has to be distinguished by the existing renormalizable FFV vertex and the flowing-in and -out goldstinos require different subroutines as in the gravitino case. We note that, in order to achieve the above simple modification, we put "G" into the end of names of each gravitino subroutine like

IORSXX → IORSGX.

References

1. G.F. Giudice, R. Rattazzi, Phys. Rep. **322**, 419 (1999)
2. K. Hagiwara, K. Mawatari, Y. Takaesu, Eur. Phys. J. C **71**, 1529 (2011)
3. K. Hagiwara, H. Murayama, I. Watanabe, Nucl. Phys. B **367**, 257 (1991)
4. H. Murayama, I. Watanabe, K. Hagiwara, KEK-Report 91-11 (1992)
5. T. Stelzer, W.F. Long, Comput. Phys. Commun. **81**, 357 (1994)
6. G.C. Cho, K. Hagiwara, J. Kanzaki, T. Plehn, D. Rainwater, T. Stelzer, Phys. Rev. D **73**, 054002 (2006)

[3] It should be noted that the effective Lagrangian (1) allow to calculate the FFV and FFVV interactions only for massless gauge bosons.

7. F. Maltoni, T. Stelzer, J. High Energy Phys. **0302**, 027 (2003)
8. J. Alwall, P. Demin, S. de Visscher, R. Frederix, M. Herquet, F. Maltoni, T. Plehn, D. Rainwaterd, T. Stelzer, J. High Energy Phys. **0709**, 028 (2007)
9. C. Cheung, Y. Nomura, J. Thaler, J. High Energy Phys. **1003**, 073 (2010)
10. T. Moroi, arXiv:hep-ph/9503210
11. T. Lee, G.H. Wu, Phys. Lett. B **447**, 83 (1999)
12. M. Bolz, A. Brandenburg, W. Buchmuller, Nucl. Phys. B **606**, 518 (2001) [Erratum *ibid.* **790**, 336 (2008)]
13. M. Klasen, G. Pignol, Phys. Rev. D **75**, 115003 (2007)
14. D.E. Morrissey, T. Plehn, T.M.P. Tait, arXiv:0912.3259 [hep-ph]
15. D.A. Dicus, S. Nandi, J. Woodside, Phys. Rev. D **41**, 2347 (1990)
16. D.A. Dicus, S. Nandi, Phys. Rev. D **56**, 4166 (1997)
17. J. Kim, J.L. Lopez, D.V. Nanopoulos, R. Rangarajan, A. Zichichi, Phys. Rev. D **57**, 373 (1998)
18. J. Pumplin, D.R. Stump, J. Huston, H.L. Lai, P.M. Nadolsky, W.K. Tung, J. High Energy Phys. **0207**, 012 (2002)
19. A.A. Affolder (CDF Collaboration), Phys. Rev. Lett. **85**, 1378 (2000)
20. A. Brignole, F. Feruglio, M.L. Mangano, F. Zwirner, Nucl. Phys. B **526**, 136 (1998) [Erratum *ibid.* **582**, 759 (2000)]